Supporting Information

Wu et al. 10.1073/pnas.1323989111

SI Materials and Methods

Synthesis of Starting Materials. MCM-41 was synthesized hydrothermally according to the method reported by Gallis and Landry (1) using n-hexadecyltrimethylammonium bromide (99+% purity; Alfa Aesar) as structure-directing agent (SDA). Tetraethoxysilane (99+% purity; Sigma–Aldrich) was the silica source. SBA-15 samples were synthesized hydrothermally in an autoclave using BASF Pluronic P123 as SDA as described by Zhao et al. (2). SBA-15 synthesized by this method has uniform pore sizes from 5 to 10 nm, and it can be expanded up to 30 nm by an organic cosolvent such as 1,3,5-trimethylbenzene (99+% purity; Alfa Aesar) (2). The microporous pure silica zeolite sample SSZ-24 was synthesized and characterized at Chevron Energy Technology Company, Richmond, California, as described elsewhere (3).

All synthesized porous silica samples [except the zeolitic SSZ-24 where the N,N,*N*-trimethyl-1-adamantammonium iodide (TMAAI) is already clathrated within the structure during synthesis and cannot be introduced by outside addition] were calcined in a Lindberg tube furnace by heating at 1 °C/min from room temperature to 500 °C and holding at this temperature for 8 h under N_2 and another 8 h under O_2. Then the silica furnace tube was sealed under dry nitrogen, the furnace cooled, and the samples were transferred into a nitrogen-filled glove box to prevent adsorption of moisture. Before each calorimetric measurement, 8–12 mg sample pellets were pressed and sealed in small vials in the glove box before transferring to the calorimeter. TMAAI, with ^{13}C enrichment for the methyl groups for solid-state NMR experiments, was synthesized at Chevron Energy Technology Company, Richmond, California, as described elsewhere (4).

Preparation of TMAAI-Containing Porous Silica. Before loading TMAAI, all of the calcined mesoporous silica samples (MCM-41 2.2 nm and SBA-15 6.6, 12.8, and 20.0 nm) were activated under vacuum at 200 °C overnight to maximize removal of adsorbed species. The glass vials containing the mesoporous silicas in impregnation experiments were preheated at 120 °C for 12 h to remove adsorbed H_2O. A solution of TMAAI was prepared by mixing 1.0 g of TMAAI powder with 25 mL of chloroform (99.9+% purity; Alfa Aesar). This solution was stored in a Teflon fluorinated ethylene propylene chloroform-resistant container. TMAAI-containing mesoporous silica samples were prepared by an incipient wetness impregnation method described earlier (5). The loading process included eight successive impregnations of 0.50 g of each mesoporous silica sample with a small amount of the TMAAI solution, which was equal to the total pore volume of 0.50 g silica sample, allowing the silica to just be wetted. Between each impregnation, the solvent was removed by heating at 120 °C overnight. After eight impregnation experiments, all TMAAI-containing mesoporous silica samples were evacuated at 120 °C overnight and transferred to a dry nitrogen-filled glove box to avoid moisture. SSZ-24 has TMAAI occluded as its original SDA.

Characterization. Nitrogen adsorption/desorption isotherms on all calcined mesoporous silica samples were performed on a Micromeritics ASAP 2020 instrument at liquid nitrogen temperature (−196 °C). The samples were degassed at 200 °C overnight to maximize H_2O removal before any isotherm analyses. The Brunauer–Emmett–Teller equation and the Barrett-Joyner-Halenda methods (6, 7) were used to derive the surface areas and pore structures.

Thermogravimetric (TG) analysis on as-made SSZ-24 and TMAAI-containing mesoporous silica samples was carried out using a Netzsch STA 449 (Netzsch GmbH) to determine the total organic contents in TMAAI-containing porous silicas. In the TG analyses, about 10 mg sample was put in a platinum crucible, which was heated from 30 °C to 1,200 °C in airflow at 10 °C/min. Buoyancy corrections were made by running an empty platinum crucible under the same experimental condition. Experiments on each sample were repeated at least twice to ensure reproducibility.

Two sets of differential scanning calorimetry (DSC) measurements were performed. The first group used a Netzsch STA 449 system (Netzsch GmbH). The TMAAI-containing mesoporous sample was placed in a platinum crucible which was heated from 30 °C to 320 °C in argon. The same amount of calcined mesoporous silica was used as reference. The second type of DSC tests were carried out using a Netzsch DSC 404 (Netzsch GmbH) to investigate possible changes of motion for molecular TMAAI confined in mesoporous silica at low temperature (40 to −80 °C in helium). All of the DSC experiments were programmed with a heating/cooling rate of 10 °C/min.

Powder X-ray diffraction (XRD) patterns of calcined mesoporous silica samples were collected by an Inel X-ray diffractometer XRG 3000 (Inel Inc.) operated at 30 kV and 30 mA, using Cu $K\alpha$ radiation (λ = 1.5406 Å) with a Ni filter to identify mesoporous silica framework phases. Data were collected at 0.5–100° (2θ). The XRD patterns of TMAAI-containing mesoporous silica samples were collected using the same instrument (2θ range 0.5–100°). The nanocrystal sizes of TMAAI in the pores of mesoporous silicas were calculated from peak broadening using Scherrer formula via Rietveld refinement implemented in JADE software (Jade v6.11, 2002; Materials Data Inc.).

Infrared (IR) spectra of calcined and TMAAI-containing porous silica samples, including calcined and as-made SSZ-24 (mixed with KBr in 1:100 wt/wt ratio), were recorded from 400 to 4,000 cm^{-1} using a Bruker Equinox 55 FTIR spectrometer (Bruker Optics Inc.).

TMAAI-containing porous silica samples were opened in a glove box filled with Ar and loaded into 4-mm ZrO_2 rotors for solid-state NMR experiments. Dry N_2 gas was used for sample spinning, and the spinning rates are reported at the upper corner of each NMR spectrum. The ^1H and ^{13}C MAS spectra with ^1H decoupling were all recorded at room temperature using a Bruker DSX 500-MHz spectrometer (Bruker Corporation) and a Bruker 4-mm cross-polarization magic angle spinning (CPMAS) probe. Variable temperature MAS experiments were followed in the range of −90–140 °C using a 300-MHz spectrometer equipped with a Tecmag Discovery console and a 4-mm Bruker CPMAS probe. The ^1H and ^{13}C spin–lattice relaxation times under MAS condition were measured using an inversion-recovery pulse sequence (8) with 4 and 8 μs-π/2 and π pulses, respectively (with 10 min of thermal equilibration). The fitting of temperature-dependent T_1 data was performed using the T_1^{-1} equation of Bloembergen–Purcell–Pound (9) theory with contributions from both ^1H–^1H and ^1H–^{13}C dipole–dipole couplings taken into account as the principal relaxation source. From the correlation time of molecular motion and the Arrhenius relation, $\tau_D^{-1} = \tau_o^{-1}\exp(-E_a/k_BT)$, the activation energy E_a of molecular motion was extracted from the optimal fit at two different magnetic fields, 7 and 11.7 T.

Hydrofluoric acid (HF) solution calorimetry used a Setaram C-80 Calvet twin microcalorimeter (Setaram Instrumentation) equipped with HF-resistant reaction cells developed by Piccione et al. (10). Sample pellets (~10 mg) were placed into a small

plastic plug and pushed downward into the solvent [25 wt % aqueous HF (5.4 g at 50 °C)] by a retractable rod. The same amount of deionized water was placed into the reference cell. TMAAI solutions in 25 wt % aqueous HF were preadded into the HF solvent for the dissolution of the calcined porous silica to balance the thermodynamic cycle described below.

Although it was not possible to stir during the reaction, the equilibration of sample dissolution in aqueous HF was confirmed by the return of the calorimeter baseline. Three to four succeeded measurements were performed on each sample to ensure reproducibility. Blank runs were also performed to determine the heat effect of pushing the rod.

The enthalpy of interaction at 50 °C between porous silica, including SSZ-24, and TMAAI in their dilute ion in aqueous HF solution reference state can be calculated from the following thermochemical cycle. The interaction at 50 °C between TMAAI and silica is described by reaction **S1**, in which n is the number of moles of TMAAI confined in one mole of porous SiO_2:

$$SiO_2(s) + n\text{TMAAI}(\text{aq HF}) = SiO_2(\text{TMAAI})_n\,(s). \qquad \textbf{[S1]}$$

The enthalpy defined in reaction **S1** can be derived from reactions **S2** and **S3**:

$$SiO_2(s) + n\text{TMAAI}(\text{aq HF}) = SiO_2(\text{aq HF}) + n\text{TMAAI}(\text{aq HF}) \qquad \textbf{[S2]}$$

$$SiO_2(\text{aq HF}) + n\text{TMAAI}(\text{aq HF}) = SiO_2.(\text{TMAAI})_n(s). \qquad \textbf{[S3]}$$

$\Delta H_1 = \Delta H_2 + \Delta H_3$. The enthalpies ΔH_2 and $-\Delta H_3$ are identical to the measured enthalpies of solution for calcined and TMAAI-containing porous silica samples, respectively. Here (s) means solid at room temperature, and (aq HF) refers to the dissolved state in aqueous hydrofluoric acid at 50 °C. This methodology is the same as that used by Piccione et al. (10) and Trofymluk et al. (11) in their study of silica–organic interactions. TMAAI was present in the HF solution into which the calcined mesoporous silica dissolved to ensure the same dissolved state for both the organic-containing and organic-free silica.

1. Gallis KW, Landry CC (1997) Synthesis of MCM-48 by a phase transformation process. *Chem Mater* 9(10):2035–2038.
2. Zhao DY, Huo QS, Feng JL, Chmelka BF, Stucky GD (1998) Nonionic triblock and star diblock copolymer and oligomeric surfactant syntheses of highly ordered, hydrothermally stable, mesoporous silica structures. *J Am Chem Soc* 120(24):6024–6036.
3. Bialek R, Meier WM, Davis M, Annen MJ (1991) The synthesis and structure of Ssz-24, the silica analog of Alpo4-5. *Zeolites* 11(5):438–442.
4. Zones SI (1991) Conversion of Faujasites to High-Silica Chabazite SSZ-13 in the Presence of N,N,N-Trimethyl-1-Adamantammonium Iodide. *J Chem Soc Faraday T* 87(22):3709–3716.
5. Regalbuto J (2007) *Catalyst Preparation: Science and Engineering* (CRC, Boca Raton, FL).
6. Brunauer S, Emmett PH, Teller E (1938) Adsorption of gases in multimolecular layers. *J Am Chem Soc* 60(2):309–319.
7. Barrett EP, Joyner LG, Halenda PP (1951) The determination of pore volume and area distributions in porous substances. 1. Computations from nitrogen isotherms. *J Am Chem Soc* 73(1):373–380.
8. Vold RL, Waugh JS, Klein MP, Phelps DE (1968) Measurement of spin relaxation in complex systems. *J Chem Phys* 48(8):3831–3832.
9. Bloembergen N, Purcell EM, Pound RV (1948) Relaxation Effects in Nuclear Magnetic Resonance Absorption. *Phys Rev* 73(7):679–712.
10. Piccione PM, et al. (2000) Thermochemistry of pure-silica zeolites. *J Phys Chem B* 104 (43):10001–10011.
11. Trofymluk O, Levchenko AA, Navrotsky A (2012) Mesoporous silica synthesis: Energetics of interaction between framework and structure directing agent. *Microporous Mesoporous Mater* 149(1):119–125.

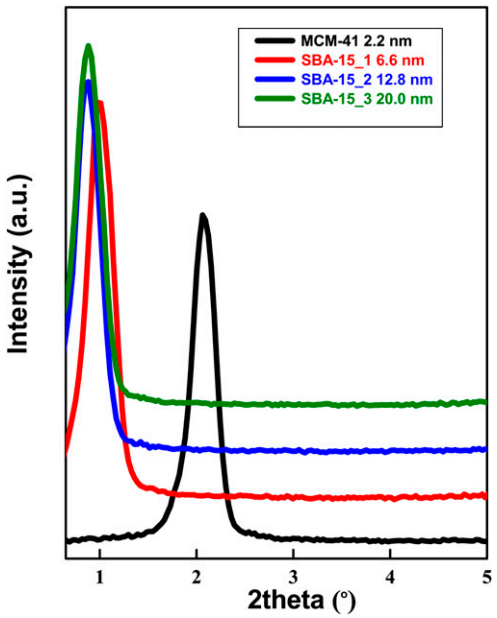

Fig. S1. Powder X-ray diffraction patterns of all mesoporous silica samples in this work (after calcination at 500 °C).

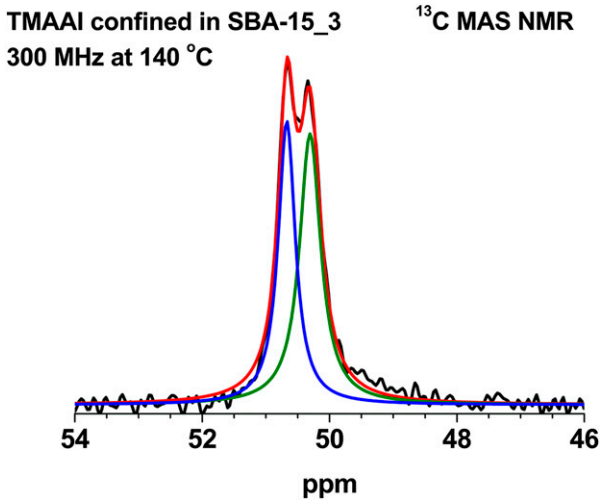

Fig. S2. The ^{13}C MAS NMR spectrum at 140 °C of TMAAI confined in 20.0-nm pore of SBA-15_3 and spectral decomposition into the amorphous and the nanocrystalline peaks, proving that the ratio of peak intensity does not change upon heating (1:1.2).

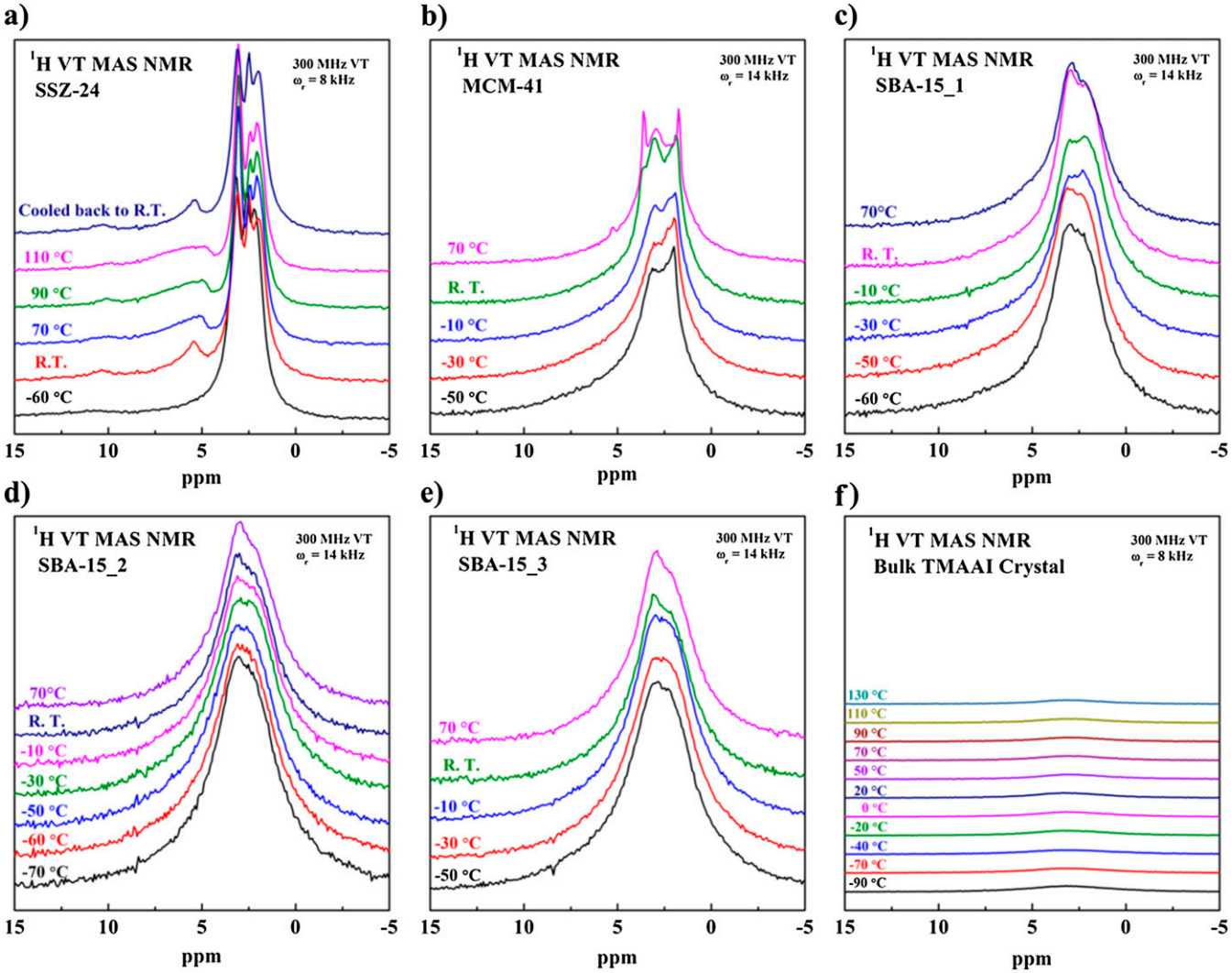

Fig. S3. The ^{1}H MAS NMR spectra for TMAAI-containing porous silicas as a function of temperature, from –90 to 140 °C. (*A*) SSZ-24, (*B*) MCM-41, (*C*) SBA-15_1, (*D*) SBA-15_2, (*E*) SBA-15_3, and (*F*) bulk TMAAI crystal. All of the figures were plotted under the same scale. Experimental conditions are marked on each spectrum.

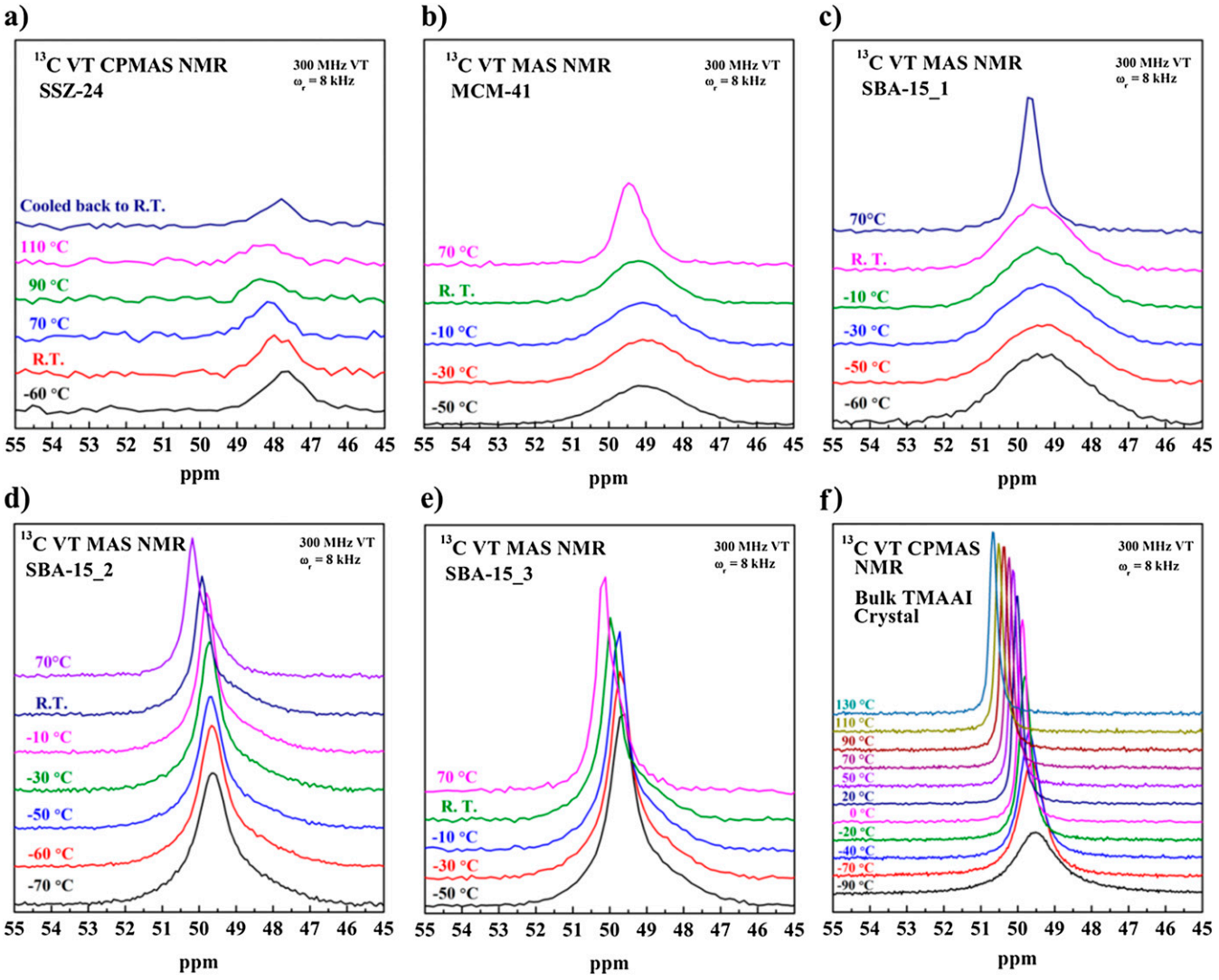

Fig. S4. The ^{13}C CPMAS NMR spectra for TMAAI-containing porous silicas as a function of temperature, from −90 to 140 °C. (*A*) SSZ-24, (*B*) MCM-41, (*C*) SBA-15_1, (*D*) SBA-15_2, (*E*) SBA-15_3, and (*F*) bulk TMAAI crystal. All of the figures are plotted under the same scale except *A*, which is zoomed in 10 times for clarity. Experimental conditions are marked on each spectrum. The methyl group of TMAAI for as-made SSZ-24 is not ^{13}C enriched; therefore, its ^{13}C signal is weaker.

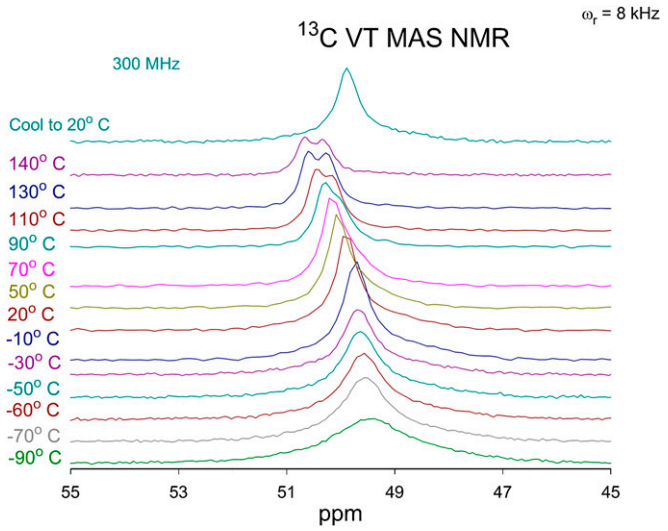

Fig. S5. The ^{13}C VT MAS NMR spectrum of TMAAI confined in SBA-15_3 (20.0 nm) as a function of temperature, from −90 to 140 °C.

Table S1. TMAAI-containing porous silica sample compositions by TGA analyses

Sample ID	Wt % water loss	Wt % TMAAI loss	% volume fraction	Molar formula of TMAAI-containing SiO_2 (TO2 basis)
TMAAI-SSZ-24	0.36	12.89	100	SiO2·**0.028**TMAAI·**0.014**H_2O
TMAAI-MCM-41	0.63	18.41	25.58	SiO2·**0.043**TMAAI·**0.026**H_2O
TMAAI-SBA-15_1	0.58	27.31	21.01	SiO2·**0.071**TMAAI·**0.027**H_2O
TMAAI-SBA-15_2	0.67	35.46	18.34	SiO2·**0.104**TMAAI·**0.035**H_2O
TMAAI-SBA-15_3	0.83	40.89	16.55	SiO2·**0.131**TMAAI·**0.048**H_2O

Table S2. Enthalpies of solution for calcined and TMAAI-containing porous silica samples in 25 wt % HF aqueous solutions at 50 °C

Framework host	Guest molecule	ΔHsol calc-SiO_2, kJ/mol SiO_2	ΔHsol TMAAI/SiO_2, kJ/mol SiO_2
SSZ-24	TMAAI	−147.51 ± 0.31	−142.62 ± 0.28
MCM-41	TMAAI	−155.99 ± 0.32	−152.78 ± 0.29
SBA-15_1	TMAAI	−162.48 ± 0.58	−158.57 ± 0.16
SBA-15_2	TMAAI	−164.27 ± 0.89	−151.65 ± 0.61
SBA-15_3	TMAAI	−166.36 ± 0.91	−147.20 ± 0.52